DESIGN AND ANALYSIS OF FOUR-LEGGED WALL-CLIMBING ROBOT

Weiyan Shang[1,2] Canjun Yang[2*] and Faju Qiu[3]
Department of mechanical engineering, Ningbo University of Technology, Ningbo 315000, China.
Corresponding author: Canjun Yang
Email: ycj@zju.edu.cn

ABSTRACT: *In order to improve the crawling ability of metal pipe wall crawling robot, a four-legged pipe wall crawling robot was designed. Based on electromagnetic adsorption test, a foot mixing electromagnetic adsorption and vacuum adsorption was designed. Establishing the leg kinematics model and motion analysis, the controlling parameters of leg motions were obtained. Finally the physical prototype was established, then the single leg exercise experiment and squatting experiment was carried out, and the leg movement posture was verified.*

KEYWORDS: *Wall-climbing Robot, Four legged robot, Kinematic model, Simulation analysis*

1. INTRODUCTION

The underwater wall autonomous mobile platform, also known as the wall-climbing robot, refers to the automated robot that can climb and complete work on vertical walls. Work on vertical walls exceeds human limits, so it is also called extreme working robot abroad. In recent years, wall-climbing robot has become a more and more important automatic mechanical device for working aloft. Japan has developed rapidly in the research of wall-climbing robot, and similar research has been carried out in China since the 1990s. The wall-climbing robot is mainly used to conduct flaw detection or painting treatment on cylindrical large tanks in petrochemical enterprises, or to clean and spray buildings. It can be used to conduct thickness measurement in the nuclear industry, and can also be used in industries such as fire protection and shipbuilding.

2. RESEARCH STATUS

2.1 Tracked Wall-climbing Mechanism

The Magneticcrawle, a magnetically absorbing crawler developed in Canada also uses the permanent magnetic tracked mechanism, as shown in Figure 1. The device is a double track mechanism that can work at a depth of 30m under water. It can crawl on vertical steel plates and carry out TV inspection on tanks and pressure vessels, etc.

S. Hagen et al. of America have developed a wall-climbing robot of electromagnetically absorbing crawler type, as shown in Figure 2 [1]. The planetary gear-driven crawler mechanism is used in the robot, and a bimetallic rotary clutch is used to control the distribution of magnetic lines of force and control the crawler disk to generate sufficient magnetic adsorption force. The robot is with visual and ultrasonic sensors for wall inspection. This type of crawler structure has strong obstacle resistance and complex terrain adaptability. However, the overall structure is relatively cumbersome and complex, and there is difficulty in steering like other types of crawler adsorption structures.

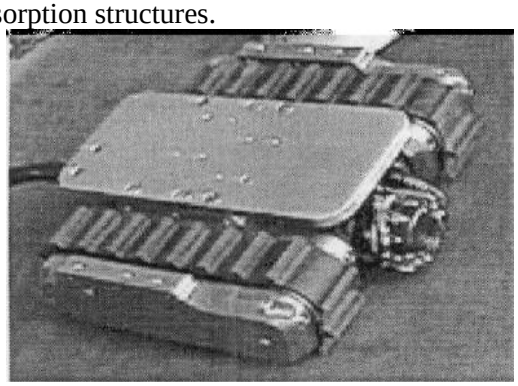

Fig. 1 Electromagnetically adsorbing crawler

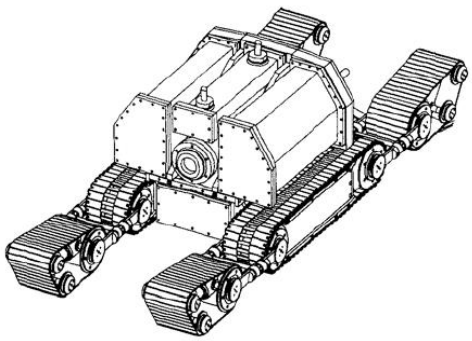

Fig. 2 Wall-climbing robot of electromagnetically adsorbing crawler type

2.2 Legged Wall-climbing Walking Mechanism

School of Mechanical Engineering Sungkyunkwan University in South Korea designed a four-legged wall-climbing robot, MRWALLSPECT-III, and completed the ground-to-wall walking test, as shown in Figure 3 [2]. There are three active joints and one passive ankle joint in each leg. The active joint is driven by a DC motor, and the passive joint is a ball joint with three rotational degrees of freedom. Three vacuum suckers are installed symmetrically for each ankle of the robot, and six vacuum suckers are installed at the bottom of the body. These suckers generate adsorption force under the action of the vacuum pump.

Balaguer.C et al. designed the ROMA wall-climbing robot, as shown in Figure 4 [3]. The ROMA-II has two feet, each with a small sucker, which ensures the reliable adsorption on rough and uneven walls. The robot can perform inspection in a complex three-dimensional environment, freely control the system for autonomous movement, and plan the optimal path to travel in real time to ensure a stable state and obstacle avoidance, and it can be controlled by the ground remote control device.

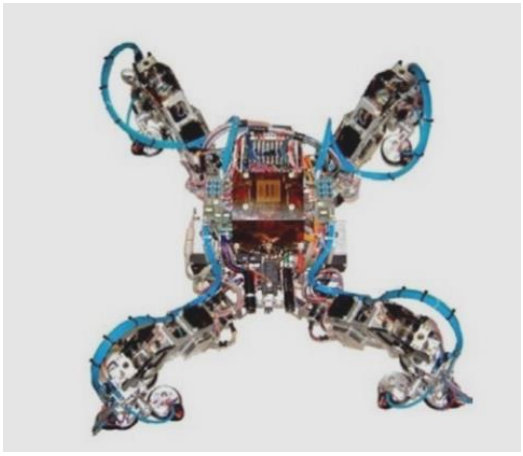

Fig. 3 Wall-climbing robot, MRWALLSPECT-III

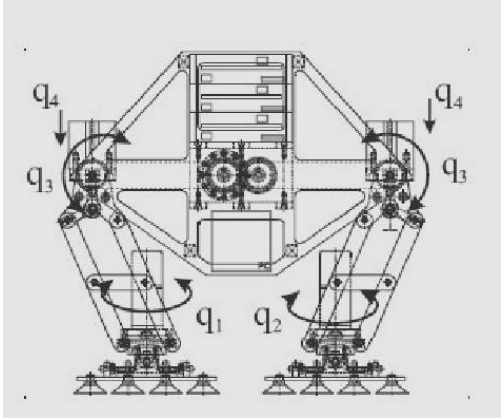

Fig.4 ROMA wall-climbing robot

The legged walking robots of the above two structures have better complex surface adaptability, but the adsorption mode of the vacuum sucker is only suitable for the air environment, so it has certain limitations for the work of oil drilling platform cleaning in the underwater environment.

By comparison and the combination with the characteristics of the working environment of the robot, the simple adsorption method is difficult to adapt to the unstructured oil platform cleaning operation. Therefore, the vacuum adsorption and magnetic adsorption are combined in the design to complete the adsorption task of the underwater operation platform.

Hammelmann of Germany developed a vacuum-adsorption, wheeled and motor-driven ship rust-removing wall-climbing robot (Figure 5) [4]. With the cleaner as the frame, it has simple and compact structure, and the diameter of the cleaner is large; the cleaner accounts for a large weight ratio of the robot, and the frame load is obviously reduced. In addition, the vacuum of the cleaner is used to recover the negative pressure so as to achieve vacuum adsorption. The robot is driven by double-driven wheel motor so that it can move freely on complex ship walls.

Fig. 5 Spiderjet3000

HydroCat is a new product launched by US's Ferro Co. that has realized automated high-pressure water cleaning. It adopts vacuum adsorption, which can derust 93m2 every time and has high rust removal efficiency. It adopts all-round steering, and weighs 79.5kg, as shown in Figure 6 [5].

The M3500 was developed by National Aeronautics and Space Administration (NASA) and the California Institute of Technology Jet Propulsion Laboratory (NASA-JPL), as shown in Figure 7. Its walking speed is up to 51cm/s, and it can walk on the surface of the paint layer with a

thickness of 6.3mm. The body mass is 222kg, the derusting width is 268mm, the derusting speed is 268m2/h, and the derusting effect is Sa2.5. M3500 adopts a combination of permanent magnet and vacuum adsorption, and it has strong adsorption capacity. The split structure makes it flexible in steering, and the differential device is designed in the transmission system to realize straight driving under the condition of single-side obstacles. The vehicle body adopts titanium alloy frame structure, which can not only protect against corrosion but also reduce weight.

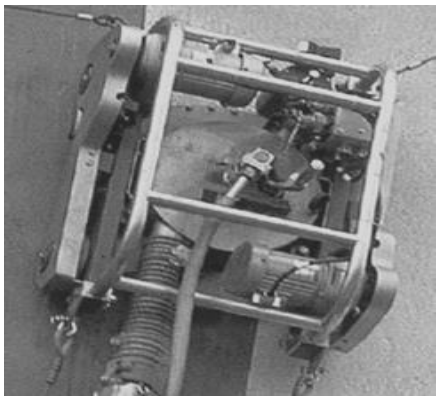

Fig. 6 HydroCat of US's Ferro Co.

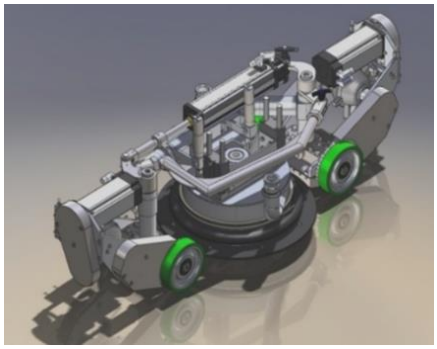

Fig. 7 NASA—JPL M 3500 Cleaning robot

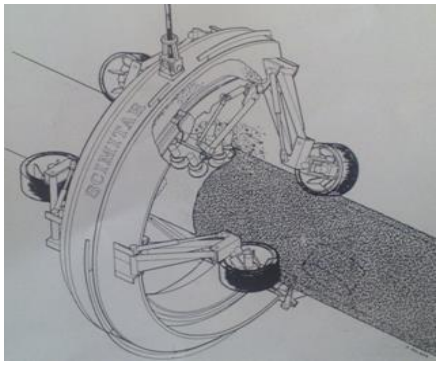

Fig. 8 "Short curved knife" (SCIMITAR) structure for cleaning up the ocean

The following problems exist in M3500: 1) It is suitable for oversized-diameter pipe walls; for small-diameter pipe walls, the four wheels need to maintain the contact with the pipe wall at the same time, a reasonable suspension system must be designed, and the wheel attitude adjustment device must be designed, which will increase the complexity of the device structure:2) the overall structure is relatively complex. By comparison, it is found that the tracked walking mechanism has better wall adaptability, but there are often complex defects in the overall structure; the legged walking system has the best complex environment adaptability, but it needs to solve the adsorption problem of the feet and complex wall and to achieve the coordinated control of each leg.

It is difficult for the wheel-enclosed robot to successfully complete tasks when moving across flanges and pipelines, as shown in Figure 8. Therefore, this structure scheme will not be adopted. The simple wheel structure usually adopts permanent magnet adsorption. Due to the limited contact area, the adsorption force will often be affected. However, if the wheeled type is combined with vacuum adsorption, it is expected to adapt to the unstructured underwater cleaning environment.

The tracked structure scheme, legged structure scheme and wheeled mixed adsorption scheme will be compared in detail in the follow-up study.

3. STRUCTURE DESIGN OF FOUR-LEGGED ROBOT

Legged robot has the best complex environment adaptability. For the oil drilling platform, there are not only unevenness on the wall of a single pipe, but also uneven structure of the intersection position of adjacent pipe walls (especially when the diameter of the pipe wall is large). In addition, considering that the robot need to frequently turn while walking to complete the overall cleaning during the operation, the legged walking system will be selected to better adapt to the cleaning environment of the drilling platform. Legged robots can be mainly divided into the eight-legged, six-legged, four-legged, etc. Among them, the four-legged walking robot has flexible movement and good stability, which can not only realize the walking on uneven ground and complex terrain by static walking, but also realize high-speed walking by dynamic walking[6-8]. Therefore, this project selects the four-legged robot as the structure scheme for the moving system of the cleaning robot of the oil drilling platform, and carries out detailed structural design and control. The structure scheme for establishing the four-legged underwater cleaning robot is shown in Figure 9.

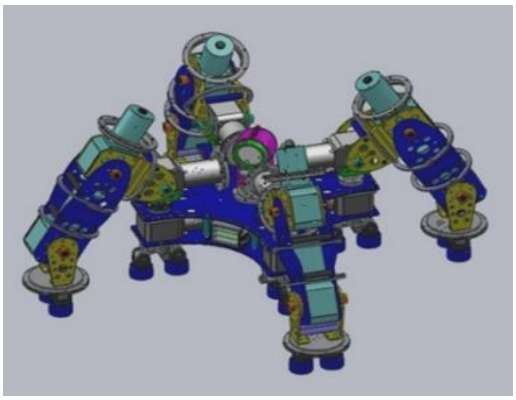

Fig. 9 Outline scheme of the four-legged robot

3.1 Legged Structure Scheme

The four-legged underwater robot consists of the body, legs, soles and camera system. It has four legs, which are identical in structure, and each consists of two parts, the leg and the sole. One end of the leg is fixedly connected to the sole of the foot through the aluminum alloy plate, and the other end is fixedly connected to the upper plate of the body. The leg of the robot consists of four rotating joints, and the movement at each joint is driven by an independent steering gear, thus forming four active degrees of freedom, and allowing the legs to move in a vertical plane under the drive of the steering gear and rotate around a vertical axis.

Since the four-legged underwater robot needs to crawl on the arc-shaped outer wall of the oil pipeline, it is necessary to specially design the sole of the robot. According to the characteristics of the working environment, the following two aspects need to be paid attention to in the design of the sole

① The outer surface of the oil pipeline is coated with protective paint, and there may also be cleaned impurities, which makes the electromagnet not fit well with the outer surface of the oil pipeline, thereby greatly reducing the adsorption force;

② Only when the center line of the two electromagnets is parallel to the cross section of the oil pipeline, will this structure has a good passive adaptation to the arc-shaped outer surface of the oil pipeline, which greatly reduces the flexibility of the robot.

Based on the two problems above, the adsorption mode of the robot's sole is changed from pure electromagnetic force adsorption to the composite adsorption of electromagnetic force and negative pressure, and the flexible structure is designed to improve the environment adaptability of the sole.

3.2 Electromagnetic Adsorption and Vacuum Adsorption Experiment

In order to better adapt to the underwater metal wall environment and grasp the electromagnetic adsorption characteristics, a preliminary electromagnetic adsorption experiment was carried out. Firstly, the electromagnet is analyzed and calculated by the ansof simulation software to obtain the influence of different contact gaps on the magnetic distribution.

It can be seen from the comparison chart that the presence of impurities leads the magnetic lines of force to become sparse. Therefore, the paint coat on the surface of the cleaned wall also affects the adsorption effect. In order to obtain the law of the influence of the thickness of the impurity layer on the magnetic adsorption force, an experimental test is conducted for the selected electromagnet.

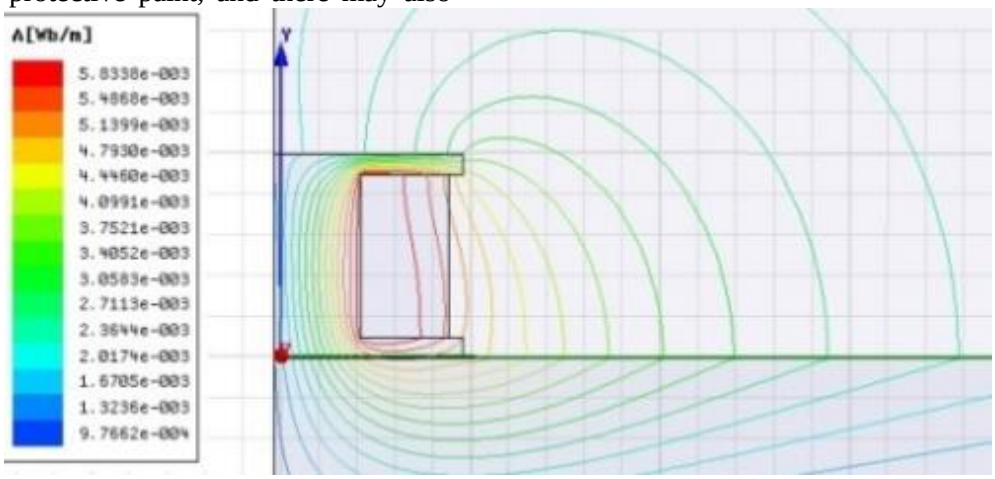

Fig. 10 Distribution of magnetic field lines without the action of impurities

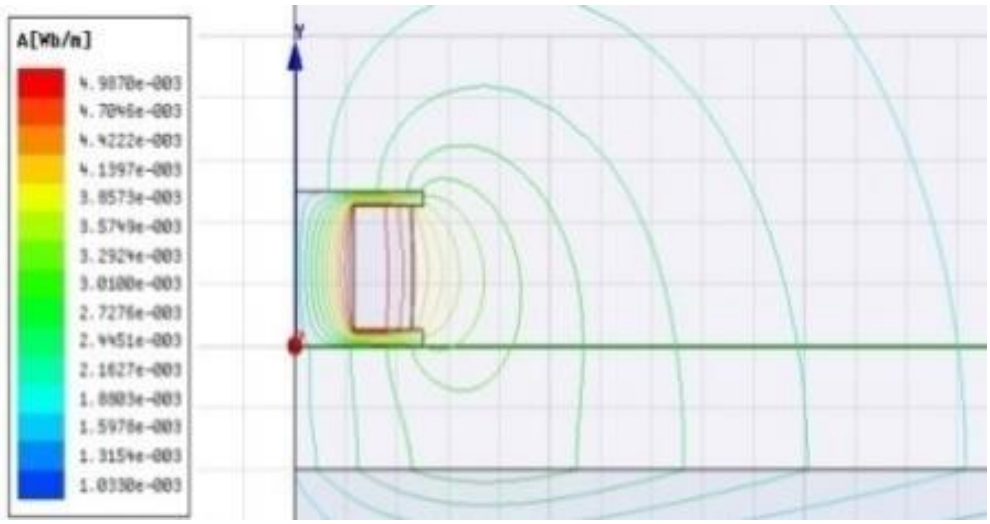

Fig. 11 Distribution of magnetic lines without the action of impurities

The influence experiment of the horizontal contact surface gap and curved surface experiment are shown in Figure 12 and Figure 13, respectively.

Fig. 12 Influence experiment of the horizontal contact surface gap

Fig. 13 Critical adsorption force of electromagnet without generating normal instability

The wall-climbing robot crawls between the walls of the oil platform. Different radii of curvature will definitely affect the contact area between the electromagnet and the wall surface, thus affecting the adsorption performance. A preliminary test was performed on the two surfaces with a radius of 1000 mm and 585 mm, as shown in Figure 13. The critical adsorption force of the electromagnet without generating normal instability is shown in Table 1.

Table 1 Critical adsorption force at two different radii of curvature

No.	Diameter/ mm	Pull force/ Kgf
1	1000	>30
2	585	9.5

It can be seen from the experiment that the smaller the diameter, the greater the decrease of the adsorption capacity of the electromagnet. Therefore, the full adsorption of the adsorbed portion and the small-diameter pipe wall should be fully considered in designing the electromagnetic sole structure to compensate for the weakening of the electromagnetic adsorption force.

3.3 Structure Design of the Sole of Foot

The sole of the foot adopts a combination of electromagnetic adsorption and negative pressure, as shown in Figure 14. Two electromagnets are reduced to one, and the connection mode is changed from hinge to fixed connection; besides, three suckers are added and fixed on the same circumference centered on the electromagnet, and the fixed ports of the three suckers are connected to one electromagnetic switch valve. When adsorption is required, the electromagnetic switch valve is turned off, the movement of the sole is driven by the leg to press the sucker against the outer wall of the oil pipeline, the seawater in the sucker is squeezed out, and a pressure difference is generated inside and outside the sucker to make

the sucker tightly pressed against the outer wall of the oil pipeline; when it is necessary to turn on it, it is just required to turn on the electromagnetic switch valve, then the seawater will enter the sucker, the pressure difference will disappear, and the sole of the foot will leave the outer wall of the oil pipeline. By calculation, the negative pressure generated by a single 60mm-diameter sucker is greater than the suction force generated by a single electromagnet (i.e., greater than 500N), so the composite adsorption mode of three suckers and one electromagnet can completely meet the requirements of suction design.

The upper connecting plate is divided into a flexible mechanism, including an upper connecting plate, a lower connecting plate, a return spring and a cross hinge. The cross hinge can make the lower connecting plate deflect a certain angle relative to the upper connecting plate in any direction around the center, thereby achieving passive adaptation to the circular outer wall of the oil pipeline in multiple attitudes, so that the movement flexibility of the robot is no longer restricted; the four return springs uniformly distributed in the circumference can make the upper and lower connecting plates of the soles of the feet parallel when the soles are not in contact with the outer wall of the oil pipeline, and play a buffering role when the soles of the feet are just in contact with the outer wall of the oil pipeline.

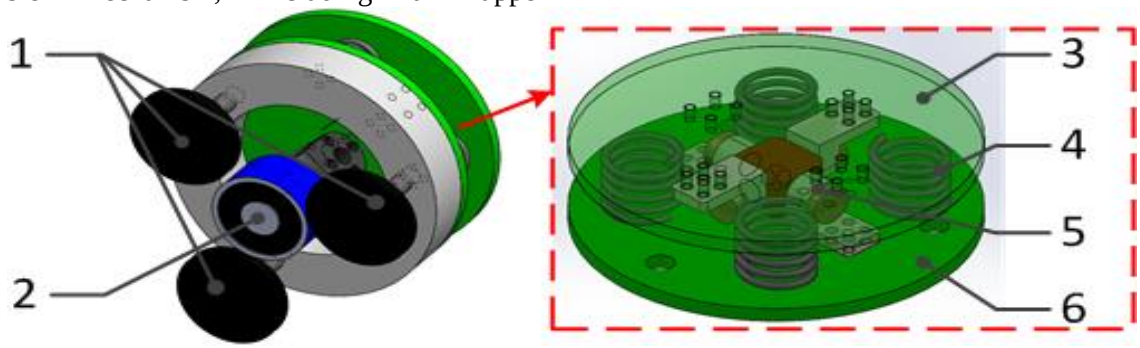

(1-sucker; 2-electromagnet; 3-upper connecting plate; 4-return spring; 5-cross hinge; 6-lower connecting plate)

Figure 14. Robot sole design

4. KINEMATICS MODELING AND SOLVING OF LEG

4.1 The establishment of Kinematics Modeling

The reference coordinate system of the three rotation joints of a single leg of the robot can be established using the D-H method, as shown in Figure 15.

The range of joint variables is shown in Table 2.

Table 2 Range of joint variables

Joint	βi	No.	αi	ai	di	θi
MP	Adduction/Abduction -90<β1<90	2(1-2)	-90°	0	123.5	β1
MP	Flexion/Extension -90<β2<90	3(2-3)	0	65	0	β2
PIP	Flexion/Extension -90<β3<90	4(3-4)	0	230	0	β3
DIP	Flexion/Extension -90<β4<90	5(4-f)	0	180	0	β4

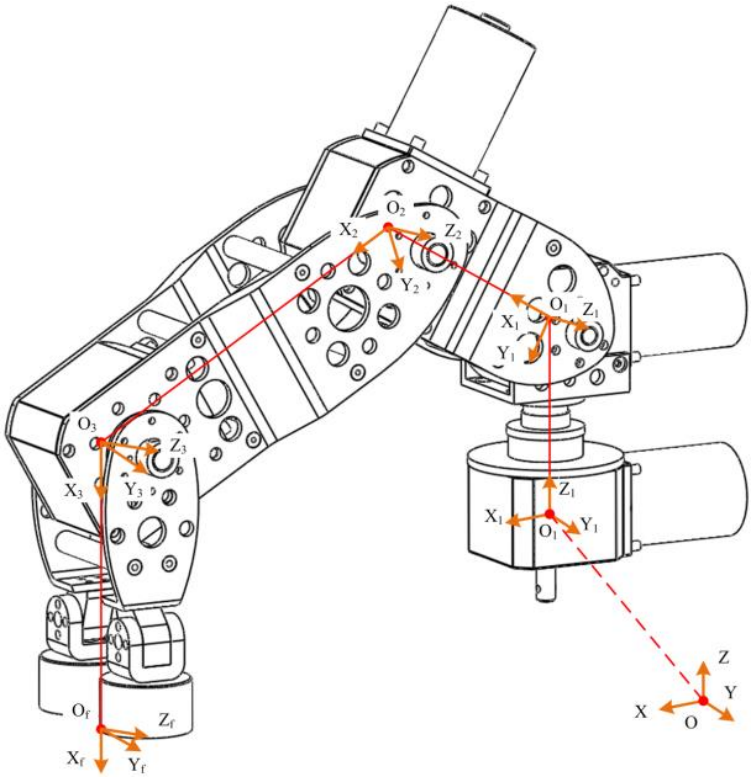

Fig. 15 Reference coordinate system of a single leg

The correct kinematics of the robot is as follows:

$$A = {}^{1}_{2}T\,{}^{2}_{3}T\,{}^{3}_{4}T\,{}^{4}_{f}T = \begin{bmatrix} c_1c_{234} & -c_1s_{234} & -s_1 & a_2c_1c_2 + a_3c_1c_{23} + a_4c_1c_{234} \\ s_1c_{234} & -s_1s_{234} & c_1 & a_2s_1c_2 + a_3s_1c_{23} + a_4s_1c_{234} \\ -s_{234} & -c_{234} & 0 & d_1 - a_2s_2 - a_3s_{23} - a_4s_{234} \\ 0 & 0 & 0 & 1 \end{bmatrix} = \begin{bmatrix} n_x & o_x & a_x & p_x \\ n_y & o_y & a_y & p_y \\ n_z & o_z & a_z & p_z \\ 0 & 0 & 0 & 1 \end{bmatrix}$$

Through solving, its inverse kinematics is.

The inverse kinematics of a single leg is obtained by simultaneous equations.

$$\begin{cases} \theta_1 = \arctan(\dfrac{p_y}{p_x}) \\ \theta_2 = \arctan(\dfrac{\gamma}{\sqrt{\alpha^2+\beta^2-\gamma^2}}) - \arctan\dfrac{\alpha}{\beta} \\ \theta_3 = \arctan\dfrac{\beta - a_2\sin\theta_2}{\alpha - a_2\cos\theta_2} - \theta_2 \\ \theta_4 = \dfrac{\pi}{2} - \theta_2 - \theta_3 \end{cases}$$

Where,

$$\begin{cases} \alpha = \sqrt{p_x^2 + p_y^2} \\ \beta = d_1 - p_z - a_4 \\ \gamma = \dfrac{\alpha^2 + \beta^2 + a^2{}_2 - a^2{}_3}{2a_2} \end{cases}$$

The spatial motion trajectory of each step is defined as a parabola, and the trajectory equation is,

$$\mathbf{X} = [x, 0, z(x)];$$

$$z(x) = -0.08(x-200)(x-260) - 143;$$

$$x \in [200, 260]$$

The attitude of each joint is obtained:

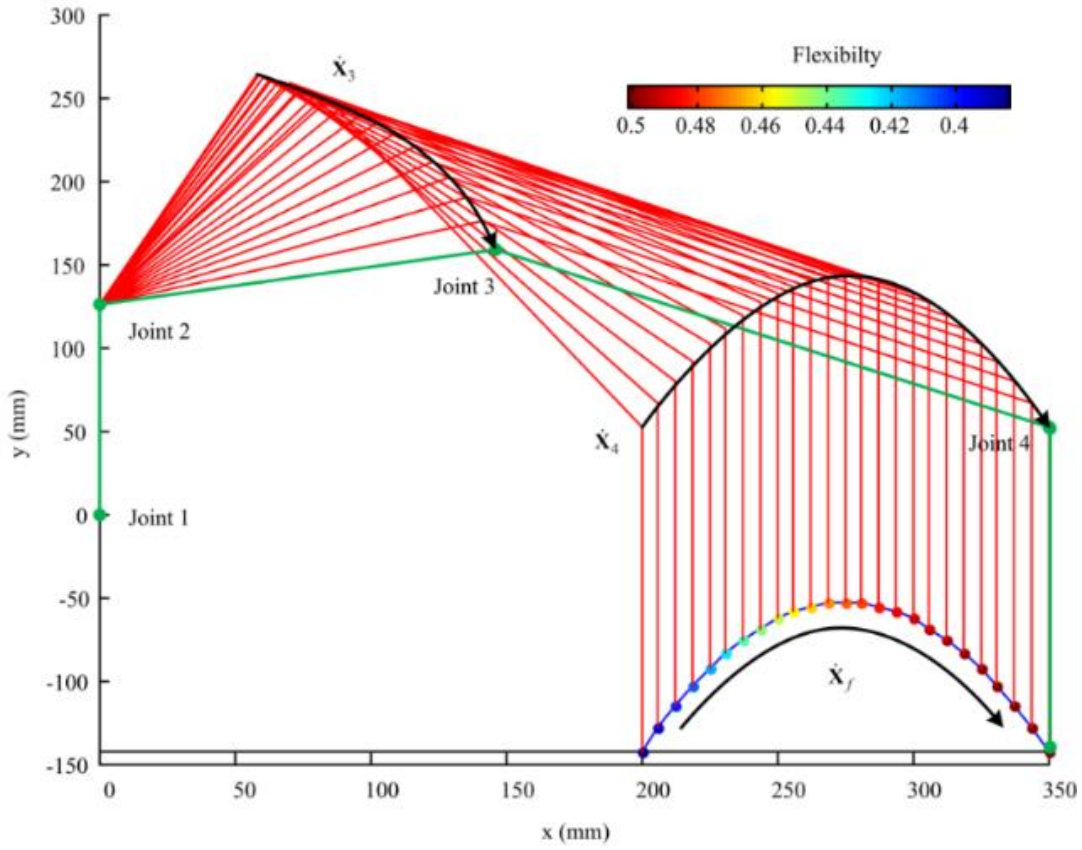

Fig. 16 Chart of the attitude of each joint

4.2 Gait Planning

For the overall robot motion, the total cycle 4TP, each phase TP, and each foot plan are defined as，

$$\mathbf{C}_A=\begin{cases}\begin{bmatrix}x_A\\y_A\\z_A\end{bmatrix}=\begin{bmatrix}-10t+350\\0\\-0.016(x_A-200)(x_A-350)-143\end{bmatrix}; & (0\le t<T_P)\\ \begin{bmatrix}x_A\\y_A\\z_A\end{bmatrix}=\begin{bmatrix}200+10(t-T_p)/3\\0\\-143\end{bmatrix}; & (T_P\le t<4T_P)\end{cases}$$

$$\mathbf{C}_B=\begin{cases}\begin{bmatrix}x_B\\y_B\\z_B\end{bmatrix}=\begin{bmatrix}200\frac{2}{3}+10\frac{t}{3}\\0\\-143\end{bmatrix}; & (0\le t<T_P)\\ \begin{bmatrix}x_B\\y_B\\z_B\end{bmatrix}=\begin{bmatrix}10(t-T_P)+200\\0\\-0.016(x_B-200)(x_B-350)-143\end{bmatrix}; & (T_P\le t<2T_P)\\ \begin{bmatrix}x_B\\y_B\\z_B\end{bmatrix}=\begin{bmatrix}350-10\frac{(t-2T_P)}{3}\\0\\-143\end{bmatrix}; & (2T_P\le t<4T_P)\end{cases}$$

$$\mathbf{C}_C=\begin{cases}\begin{bmatrix}x_C\\y_C\\z_C\end{bmatrix}=\begin{bmatrix}200\frac{2}{3}+\frac{10t}{3}\\0\\-143\end{bmatrix}; & (0\le t<2T_P)\\ \begin{bmatrix}x_A\\y_A\\z_A\end{bmatrix}=\begin{bmatrix}-10(t-2T_P)+350\\0\\-0.016(x-200)(x-350)-143\end{bmatrix}; & (2T_P\le t<3T_P)\\ \begin{bmatrix}x_C\\y_C\\z_C\end{bmatrix}=\begin{bmatrix}200+\frac{10(t-3T_P)}{3}\\0\\-143\end{bmatrix}; & (3T_P\le t<4T_P)\end{cases}$$

$$\mathbf{C}_D=\begin{cases}\begin{bmatrix}x_D\\y_D\\z_D\end{bmatrix}=\begin{bmatrix}350-10\frac{t}{3}\\0\\-143\end{bmatrix}; & (0\le t<3T_P)\\ \begin{bmatrix}x_D\\y_D\\z_D\end{bmatrix}=\begin{bmatrix}10(t-3T_P)+200\\0\\-0.016(x_D-200)(x_D-350)-143\end{bmatrix}; & (3T_P\le t<4T_P)\end{cases}$$

$$\theta_4=\pi-\alpha-\theta_2-\theta_3$$

The robot's gait is controlled based on the above analysis, and the cleaning robot's walking on the surface of pipe is completed.

4.3 Kinematics Analysis

The controlled object is shown in Figure 17, a leg structure with four degrees of freedom, in which the hip joint has two degrees of freedom, and the knee joint and the ankle joint has one degree of freedom, respectively. The D-H

coordinates shown in the figure are established, and the parameters of each joint are shown in Table 3.

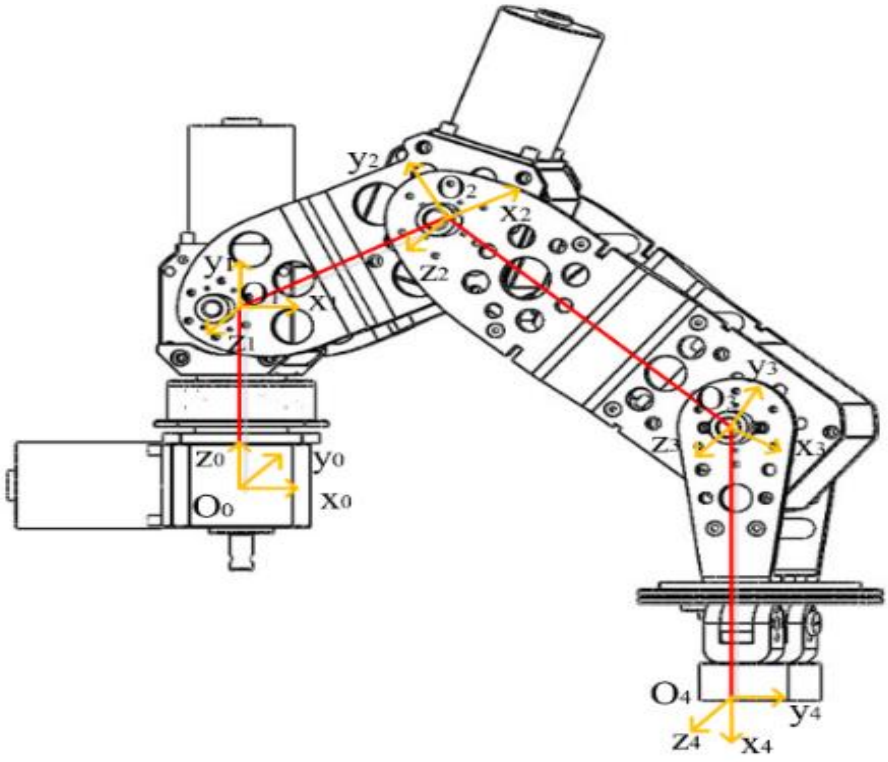

Fig. 17 Establishment of robot D-H coordinates

Table3 D-H coordinates parameters

i	l_i/mm	α_i/°	d_i/mm	θ_i/°
1	0	90	123.5	θ_1
2	65	0	0	θ_2
3	230	0	0	θ_3
4	180	0	0	θ_4

The kinematics for the robot is solved according to the established D-H coordinates, and the one-leg transformation matrix is obtained as follows.

$$ {}^{0}\mathbf{T}_{4} = \begin{bmatrix} n_x & o_x & a_x & p_x \\ n_y & o_y & a_y & p_y \\ n_z & o_z & a_z & p_z \\ 0 & 0 & 0 & 1 \end{bmatrix} \quad (1) $$

Where

$n_x = C_1C_{234}$;

$n_y = S_1C_{234}$;

$n_z = S_{234}$;

$o_x = -C_1S_{234}$;

$o_y = -S_1S_{234}$;

$o_z = C_{234}$;

$a_x = S_1$;

$a_y = -C_1$;

$a_z = 0$;

$p_x = C_1\left(l_4C_{234} + l_3C_{23} + l_2C_2\right)$;

$p_y = S_1\left(l_4C_{234} + l_3C_{23} + l_2C_2\right)$;

$p_z = l_4S_{234} + l_3S_{23} + l_2S_2 + d_1$.

During the crawling, the sole needs to be adsorbed, and the last joint of the leg needs to be perpendicular to the ground, and the qualified condition is obtained, i.e. θ_1+θ_2+θ_3=-90°. The joint angle can be inversely solved.

$$\begin{cases} \theta_1 = \arctan\dfrac{p_y}{p_x}; \\ \theta_2 = \arctan\dfrac{\sqrt{1-\cos^2\gamma}}{\cos\gamma} + \arctan\dfrac{\beta}{\alpha}; \\ \theta_3 = \arctan\dfrac{\sqrt{1-C_3^2}}{C_3}; \\ \theta_4 = -90° - \theta_2 - \theta_3. \end{cases} \tag{2}$$

Where

$$\begin{cases} \cos\gamma = \dfrac{\alpha^2+\beta^2+l_2^2-l_3^2}{2l_2\sqrt{\alpha^2+\beta^2}}; \\ C_3 = \dfrac{\alpha^2+\beta^2-l_2^2-l_3^2}{2l_2L_3}; \\ \alpha = \sqrt{p_x^2+p_y^2}; \\ \beta = p_z - d_1 + l_4. \end{cases} \tag{3}$$

Thus, the kinematics analysis of the robot is completed, providing a basis for the subsequent simulation and experiment.

4.4 Kinematics Simulation

The inverse kinematics is solved using MATLAB programming according to the kinematics model, and thereby, the motion parameter of the robot under the ideal condition in the corresponding trajectory can be obtained. This parameter can be used as the original parameter of the robot control. It is found through the experiment that the robot is in a horizontal attitude, and the adduction and abduction movements of the first joint, the hip joint, is not affected by gravity, and the trajectory following effect is good. In order to obtain a better experimental effect, the first joint is fixed, and the remaining three joints will perform a vertical linear motion which is most affected by gravity in one working plane. Taking this movement as an analysis case, the sole is arranged to reciprocate 300 mm from the body in the horizontal direction and 60 mm in the vertical direction. The position of each joint and the attitude of the robot when lifting the leg are shown in Figure 18. The theoretical values of the joint angles are shown in Figure 19. Under the ideal condition, the influence of gravity on the motion is not considered, and the leg falling is the reverse motion of the leg raising.

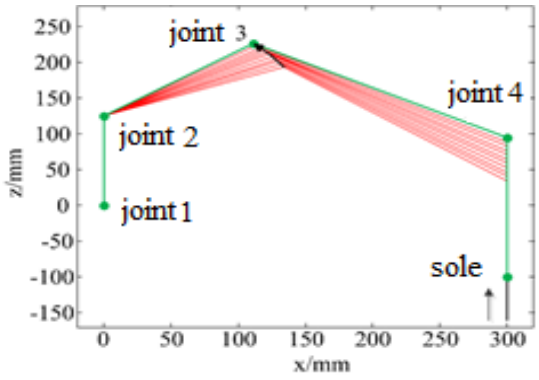

Fig. 18 Robot's attitude of vertical linear motion

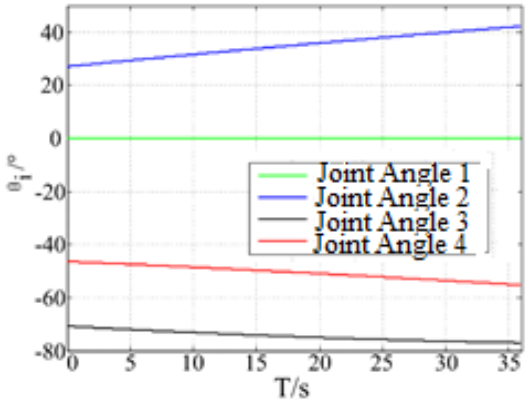

Fig. 19 Ideal joint angles of vertical linear motion

5. EXPERIMENTAL VERIFICATION

The machining of the robot's main body is completed, and the four-legged robot control system is designed, mainly including three parts: the PC, the body control module and the leg control module. The main function of the PC is that the user sends relevant directives to control the actions of the robot; it also plays the role of a monitor: the body module uploads relevant data to the PC in real time, so that it can monitor the underwater motion of the robot and related parameters in real time.

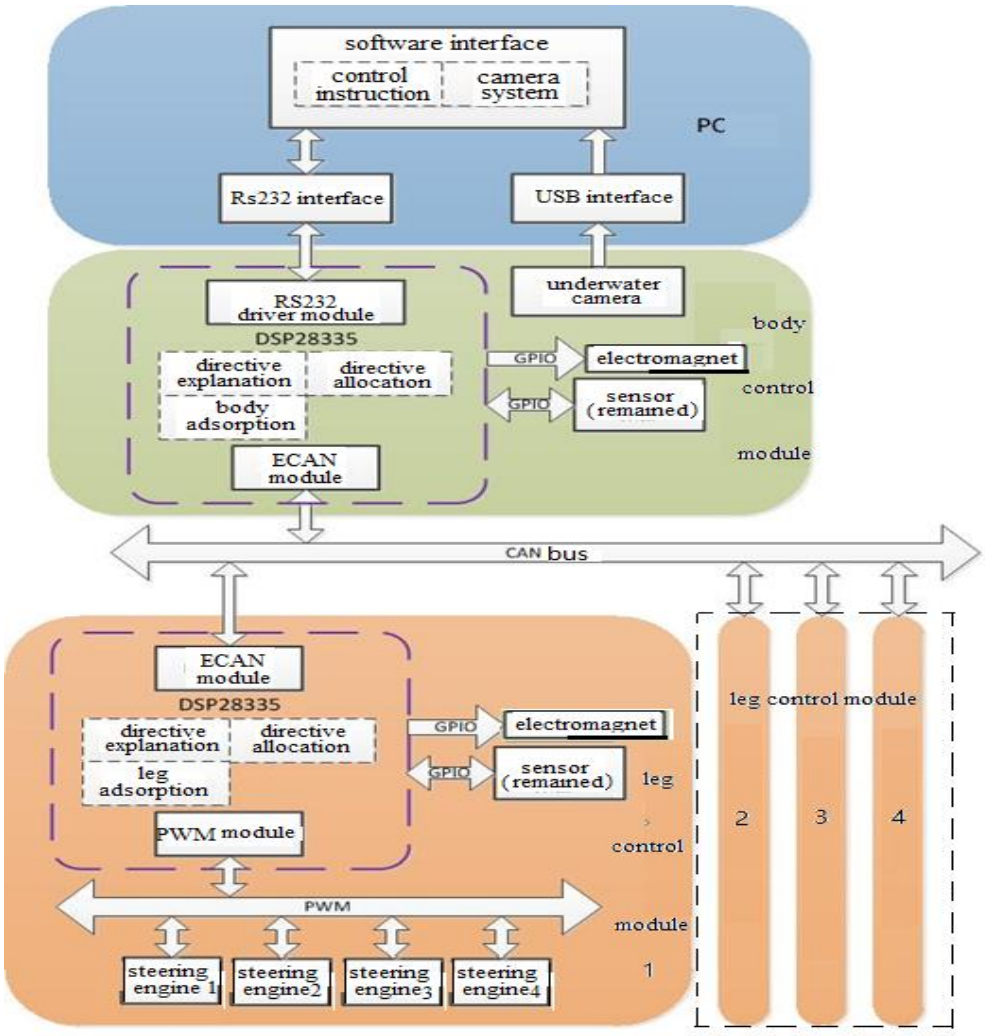

Fig. 20 The control system of four-legged robot

The robot is controlled to complete the reciprocating motions of "squatting-standing up". Except for the obvious shaking when the robot started squatting, the robot stays a stable state during the whole movement, and the coordinated movement of the legs is realized.

Using the parameters from kinematics analysis, a single leg is controlled to make movement from a low position to a high position and then from a high position to a low position, shown in figure 21. The whole movement is smooth, and except for a great shaking during the declining process, the rest of the movement is relatively stable.

Fig. 21 Single-leg movement test

Then another test of squatting-standing test was done, shown in figure 22. In this test, the four legs can move coordinately, which makes the robot complete the reciprocating action of "squatting-standing". Apart from the obvious

sway of the robot when it starts to squat, the robot is very smooth during the whole movement.

Fig. 22 Squatting-standing movement test

6. CONCLUSIONS

The following aspects are mainly studied in this paper,

(1) A four-legged wall climbing robot that can adapt to the wall environment was designed, and an electromagnetic and vacuum-adsorbing foot was carried out;

(2) The analysis and modeling of leg movement was realized, and the four joints of the legs were controlled to complete the vertical back-and-forth movement;

(3) A four-legged control system was designed, and the smoothness and steadiness of leg movement were verified through prototype test.

(4) A single leg movement and Squatting-standing movement test was done by using the parameters from kinematics analysis and the four leg robot can realize the movement as designed.

Author Contributions:

Weiyan Shang co-directed the project, wrote the manuscript, assisted with data analysis, and helped with software design and development. Faju Qiu assisted with software design and development, helped with tuning of parameters, and reviewed the manuscript. Canjun Yang co-directed the project, assisted with data analysis.

Funding:

This work was supported by NSFC Natural Science Foundation of China Research on the driving stability of undersea observation robot steering on slopes， Grant NO. 51605232. And the work was also supported by Natural Science Foundation of Ningbo Study on Steering Steady on Slope of Tracked Underwater Observation Robot, Grant NO. 010-20181JCGY01200.

Acknowledgments:

We would like to express appreciation to Bi qian and Xuelei Deng for his assistance with experiment.

Conflicts of Interest: The authors declare no conflicts of interest.

7. REFERENCES

►Hagen S. Neptune: above-ground storage tank inspection robot system. IEEE Robotics and Automation Magazine, 1995, 2(2): 9-15.

►B.L. Luk., A. A. Collie., J..Billingsley. ROBUG II: AN INTELLIGENT WALLCLIMBING ROBOT. Proceedings of the 1991 IEEE International Conferenceon Robotics and Automation Sacramento. 1991: 2342~2347.

►A. Nagakubo., S. Hirose. Walking and running of the quadruped wall-climbing robot. Proc. IEEE Int Conf on Robotics and Automation, San Diego, CA, USA, 1994: 1005~1012.

►Akinfiev T, Armada M, Nabulsi S. Climbing cleaning robot for vertical surfaces. Industrial Robot, 2009, 36(4): 352-357.

►Flow International Corporation. Hydro-Cat TM industrial cleaning system [DB/OL]. [2009- 10-20].

►Yi Zheyao, Gong yongjun. Large Wall Climbing Robot for Ship Rust Removal Cleaner. Robot.2010.10,4(32):560-566.

►Hyunsoo P., Kyung J. K. The Automated Fault-recovery for Four-legged Robots using Parallel Genetic Algorithm Original Research Article Procedia Computer Science, Volume 24, 2013:158-166.

►Petra Bin He, Zhipeng Wang, Minghe Li, and etc. Wet Adhesion Inspired Bionic Climbing Robot. Mechatronics,2014, 19(1):312-320.